



**HAL**  
open science

# CHEMICALLY-BONDED POST-INSTALLED STEEL REBARS IN A FULL-SCALE SLAB-WALL CONNECTION SUBJECTED TO THE STANDARD FIRE (ISO 834-1)

Mohamed Amine Lahouar, Nicolas Pinoteau, Jean-François Caron, Gilles Forêt,  
Thierry Guillet, Romain Mege

## ► To cite this version:

Mohamed Amine Lahouar, Nicolas Pinoteau, Jean-François Caron, Gilles Forêt, Thierry Guillet, et al.. CHEMICALLY-BONDED POST-INSTALLED STEEL REBARS IN A FULL-SCALE SLAB-WALL CONNECTION SUBJECTED TO THE STANDARD FIRE (ISO 834-1). ConSC 2017: 3rd International Symposium on Connections between Steel and Concrete , Sep 2017, Stuttgart, Germany. <hal-01617391>

**HAL Id: hal-01617391**

**<https://hal.science/hal-01617391v1>**

Submitted on 16 Oct 2017

**HAL** is a multi-disciplinary open access archive for the deposit and dissemination of scientific research documents, whether they are published or not. The documents may come from teaching and research institutions in France or abroad, or from public or private research centers.

L'archive ouverte pluridisciplinaire **HAL**, est destinée au dépôt et à la diffusion de documents scientifiques de niveau recherche, publiés ou non, émanant des établissements d'enseignement et de recherche français ou étrangers, des laboratoires publics ou privés.



HAL Authorization



# CHEMICALLY-BONDED POST-INSTALLED STEEL REBARS IN A FULL-SCALE SLAB-WALL CONNECTION SUBJECTED TO THE STANDARD FIRE (ISO 834-1)

Amine Lahouar<sup>1,2\*</sup>, Nicolas Pinoteau<sup>2</sup>, Jean-François Caron<sup>1</sup>, Gilles Forêt<sup>1</sup>,  
Thierry Guillet<sup>2</sup>, Romain Mege<sup>2</sup>

<sup>1</sup>Université Paris-Est, Laboratoire Navier Ecole des Ponts ParisTech, Marne-la-Vallée, France.

<sup>2</sup> Centre Scientifique et Technique du Bâtiment, Champs sur Marne, France

\*Corresponding Author Email: [amine.lahouar@cstb.fr](mailto:amine.lahouar@cstb.fr)

## ABSTRACT

The improvement in mechanical and adhesion properties of polymer resins allowed to progressively substitute cast-in place rebars by chemically-bonded post-installed rebars in some applications, by providing equivalent or even higher mechanical properties at ambient temperature. However, the mechanical behavior of post-installed rebars is mainly governed by the mechanical behavior of polymer resins, which are highly sensitive to temperature, addressing the topic of fire safety. In 2015, the European Assessment Document 330087-00-06.01 has been issued to harmonize the evaluation method on fire performance of these polymeric adhesives. This evaluation document proposes a fire design method allowing to ensure a sufficient bond resistance for a given duration of fire exposure before collapse.

This paper presents a full-scale fire test performed in the “Vuclain” modular gas furnace at CSTB Champs-sur-Marne (France), carried out on a 2.94 m x 2 m x 0.15 m cantilever concrete slab connected to a wall by chemically-bonded post-installed rebars and exposed to ISO fire 834-1 until failure. Experimental investigations showed that the design method presented in this paper is able to predict a time of slab collapse very close to that obtained by the fire test. The interpretation of the data collected during the fire test revealed the presence of thermal and physical phenomena responsible for the decay in the fire resistance of the post-installed rebars and therefore, responsible for the slab collapse under fire exposure.

## 1 Introduction

Post-installed rebars (PIRs) is a structural joining technique allowing the connection and the load transfer between structural elements using steel rebars and adhesive polymers<sup>1</sup>. PIRs were initially used in concrete constructions in retrofitting, extension and in repairing structures by adding new concrete sections to existing elements<sup>2,3</sup>. Over the time, the improvement in mechanical and adhesion properties of polymer adhesives have allowed to enhance the mechanical behavior of PIRs and led to achieve equivalent or even higher mechanical responses than cast-in place rebars at normal operating temperatures<sup>4,5</sup>. Thus, PIRs have gradually substitute cast-in place rebars in new constructions for

some applications by offering advantageous solutions and flexibility allowing to meet the high architectural requirements<sup>6</sup>.

However, the mechanical behavior of post-installed rebars is directly linked to the mechanical properties of polymer resins, which are highly sensitive to temperature<sup>5</sup>. Consequently, the temperature increase at the PIRs presents a potential risk affecting their safety use. Therefore, fire presents a serious hazard which should be considered when designing PIRs. Very few regulations and technical documents<sup>7,8</sup> exist today proposing methods to assess and to design the fire resistance of chemically-bonded post-installed rebars. The European Assessment Document 330087-00-06.01<sup>7</sup> is one of the most important documents existing today, proposing a fire design method for PIRs in fire situation.

This paper presents a full-scale fire test performed on “Vulcain” modular gas furnace of CSTB, carried out on a 2.94 m x 2 m x 0.15 m cantilever concrete slab connected to a wall by 8 PIRs and exposed to ISO fire 834-1<sup>9</sup> until its failure (Figure 1). The main goal is to validate a suggested design method allowing to predict the fire resistance of PIRs using characterization tests. The first part of this paper describes the test configuration and explains the design method. While, the second part presents the experimental results obtained during the fire test and compares between predicted and measured time of collapse.

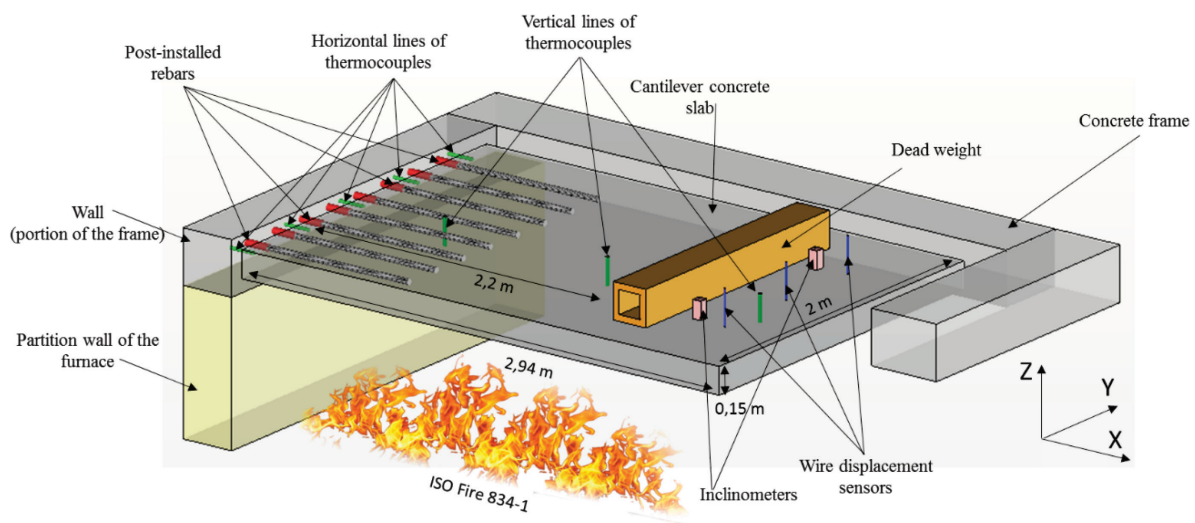


Figure 1: Vulcain fire test configuration: Instrumentation and set up on the furnace

## 2 Test specimen conception and fire resistance prediction

### 2.1 Test specimen conception

A full-scale ISO fire 834-1<sup>9</sup> test was carried out at CSTB Champs-sur-Marne on the “Vulcain” modular gas furnace. This furnace offers three possible exposure areas to perform fire tests on a horizontal configuration: 3m x 3m, 4m x 3m and 7m x 3m. The chosen configuration was 4m x 3m. The set-up of the test specimen on the furnace required the presence of a concrete frame allowing to close the furnace and to ensure its fire integrity during the test. The concrete frame was made from a C45/55 reinforced concrete and represents the wall in which post-installed rebars were anchored. The

test specimen was composed of a 2.94 m x 2 m x 0.15 m cantilever slab made from C20/25 reinforced concrete containing propylene fibers in order to avoid spalling, connected to the wall by 8 post-installed rebars chemically-bonded into concrete using epoxy resin (Figure. 1). Characterization tests were carried out on cubic concrete samples (150 mm x 150 mm x 150 mm) after 28 days of curing under ambient temperature and moisture conditions. The concrete used for the frame had a compressive strength of 58.7 MPa ( $\pm 1.3$  MPa) and a density equal to 2263 kg/m<sup>3</sup> ( $\pm 7$  kg/m<sup>3</sup>), while the concrete used for the cantilever slab had a compressive strength of 22.4 MPa ( $\pm 0.3$  MPa) and a density equal to 1987 kg/m<sup>3</sup> ( $\pm 5$  kg/m<sup>3</sup>). The number of post-installed rebars was determined according to the EC2 part 1-1 design rules<sup>10</sup> which allow a maximum spacing between bonded rebars equal to two times the thickness of the slab. The diameter of the steel rebars was 16 mm. The embedment length was set at 135 mm in order to ensure a failure by rebars sliding during the fire test. The rebars were positioned at 100 mm height in the cantilever slab, respecting the minimum concrete cover authorized by the EC2<sup>10</sup>.

A spacing of 80 mm at the sides and 200 mm at the free end of the cantilever slab was left to take into account the concrete thermal expansion and to prevent the blocking of the cantilever slab against the frame during fire test (Figure 2). This spacing between the slab and the concrete frame was filled with thermal insulation material in order to confine heat during the fire test. The slab was mechanically loaded with 325 kg dead weight positioned at 2200 mm from the wall (Figure 1). The slab weight was estimated equal to 1753 kg. The slab weight and the dead load generated a total bending moment at the wall/slab interface equal to  $M_{\text{tot}} = 32.28$  kNm. The fire test was performed after 3 months of the concrete casting.

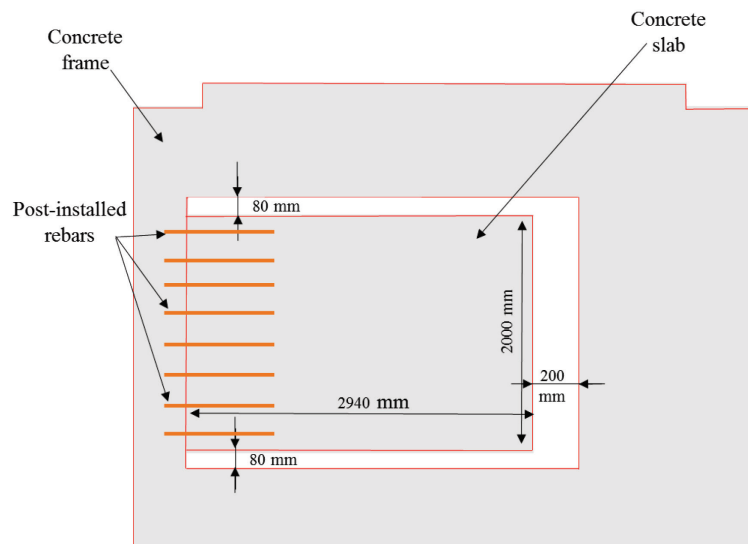


Figure 2: Position of the slab in the concrete frame

## 2.2 Prediction of the fire resistance duration

A fire design method is presented in this paper allowing to predict the fire resistance of post-installed rebars. This method relies on the knowledge and the determination of several parameters. The fire resistance calculation of PIRs using the suggested method is composed of 5 steps.

### 2.2.1 Calculation of the applied tensile load $F_{app}$

The determination of the tensile load applied on each rebar can be done either by analytical calculations or by finite element analysis. This step requires the knowledge of certain parameters such as the geometrical parameters of the slab, the concrete density, the applied mechanical load, the load position and the rebars position in the slab... The determination of the applied tensile load is based on the assumption of a uniform load distribution between the rebars. Calculations showed that for the studied configuration, the tensile load applied on each rebar is around **48 kN ( $\pm 3$  kN)**.

### 2.2.2 Thermal calculations $\theta(x,t)$

This step consists in determining the temperature distribution in the test specimen at different moments of fire exposure using thermal calculations. Thermal calculations can be done either by finite element analysis, or by analytical calculations using finite difference method by solving Fourier's equation (1). These two calculation methods require input data describing the variation of materials thermal properties ( $\lambda(\theta)$ ,  $C_p(\theta)$  and  $\rho(\theta)$ ), which can be obtained directly from the Eurocode<sup>10</sup>.

$$\rho(\theta(x,t)).C_p(\theta(x,t)).\frac{\partial\theta(x,t)}{\partial t}=\lambda(\theta(x,t)).\frac{\partial^2\theta(x,t)}{\partial x^2}+h.(\theta_{ext}(t)-\theta_{sur}(t))+\sigma.\varepsilon.(\theta_{ext}^4(t)-\theta_{sur}^4(t)) \quad (1)$$

Where  $\rho$  is the material density [ $kg/m^3$ ]

$C_p$  is the material specific heat [ $J.K^{-1}.Kg^{-1}$ ]

$\lambda$  is the material conductivity [ $W.m^{-1}.K^{-1}$ ]

$\theta(x,t)$  is the temperature of an element of the PIR at position  $x$  and at time  $t$  [K]

$h$  is the heat transfer coefficient [ $W.m^{-2}.K^{-1}$ ]

$\sigma$  is the Stefan-Boltzmann constant [ $W.m^{-2}.K^{-4}$ ]

$\varepsilon$  is the emissivity of the material

$\theta_{sur}$  is the temperature at the surface of the material [K]

At the end of this first step, a temperature map is obtained, indicating the exact temperature values at every point of the test specimen and at different moments of fire exposure. Figure 3 represents the evolution of the temperature along the embedded part of the steel rebar for different moments of fire exposure.

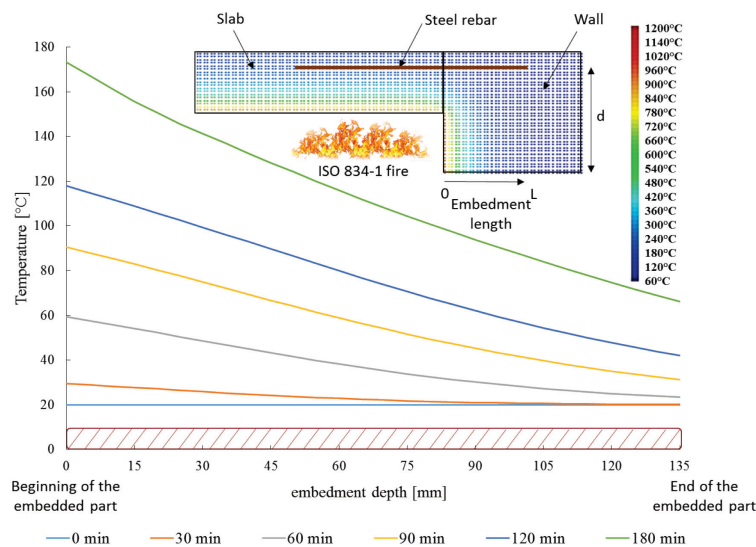


Figure 3: Evolution of the temperature along the embedded part of the steel rebar during fire test

### 2.2.3 Bond resistance-Temperature relationship $\tau_{max}(\theta)$

The bond resistance-temperature relationship is obtained by performing pull-out tests at different temperatures on post-installed rebars anchored in concrete cylinders. These tests consist in applying a constant load on the steel rebar and then heating the test specimen progressively until the extraction of the rebar (Figure. 4). This test procedure, called “pull-out tests at constant load”, provides a failure temperature for selected amounts of shear stress applied on the adhesive joint. Results obtained by pull-out tests at constant load are shown in Figure 5.

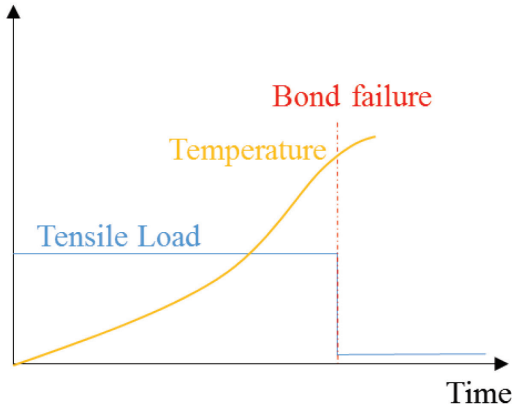


Figure 4: Test procedure of pull-out test at constant load

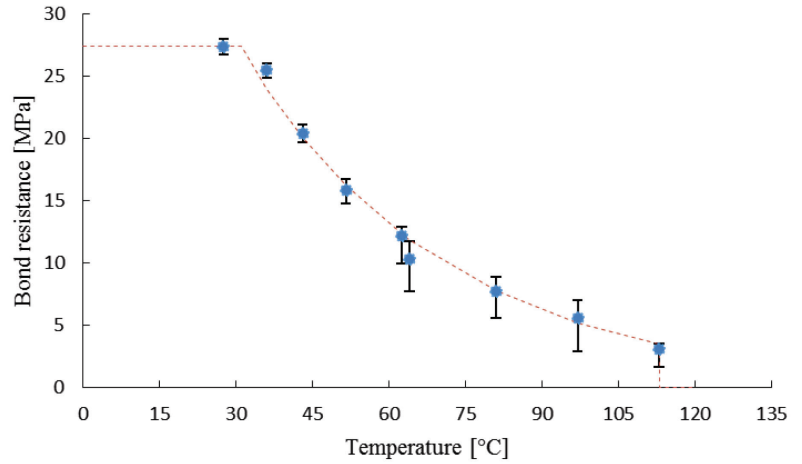


Figure 5: Results of the pull-out test campaign

### 2.2.4 Determination of the PIR bearing capacity $F_t$

The calculation of the evolution of the PIR bearing capacity during fire exposure is carried out in two stages. The first stage consists in associating a bond resistance value to each element of the bonded rebar at different moments of fire exposure by knowing the temperature evolution obtained by thermal calculations and by using the relationship bond resistance-PIR temperature (Figure 5). The second step consists in summing the bond resistance values along the embedded part of the rebar for a given moment of the fire exposure, as described by equation (2).

$$F_t = 2\pi r \int_0^L \tau_{max}(\theta(x,t)) dx \quad (2)$$

Where  $F_t$  is the load bearing capacity of the PIR at time t [N]

$r$  is the radius of the steel rebar [mm]

$L$  is the embedment length [mm]

$\tau_{max}$  is the bond resistance obtained by pull-out tests [MPa]

$\theta(x,t)$  is the temperature of an element of the PIR at position x and at time t [K].

Table 1 summarizes the evolution of the calculated bearing capacity for every 30 minutes of fire exposure.

Table 1: Evolution of the load bearing capacity of the PIR during the fire test

| Fire exposure [min] | Load bearing capacity [kN] | Applied load [kN] |    |
|---------------------|----------------------------|-------------------|----|
| 0                   | 190                        | >                 | 48 |
| 30                  | 190                        | >                 | 48 |
| 60                  | 131                        | >                 | 48 |
| 90                  | 79                         | >                 | 48 |
| 120                 | 40                         | <                 | 48 |
| 180                 | 9                          | <                 | 48 |

### 2.2.5 Time of collapse

The fire resistance design method assumes that failure occurs when the shear stress reaches the bond resistance at all the elements of the PIR. Therefore, the time collapse is considered as the time at which the PIR bearing capacity becomes equal to or lower than the applied tensile. Thus, according to calculations, the failure must occur around **120 minutes** of fire exposure.

## 3 Validation test: Full-scale fire test on a slab-wall connection

### 3.1 Metrology

#### 3.1.1 Temperature measurements

In order to study the temperature increase during the fire test, rows of thermocouples have been installed at different positions in the test specimen (Figure 1). 5 rows of thermocouples were introduced horizontally into the wall, at the same height as the rebars and positioned respectively at 111 mm, 555 mm, 1000 mm, 1450 mm and 1889 mm from the lateral side of the slab. Each row was composed of 5 thermocouples positioned respectively at 10 mm, 20 mm, 30 mm, 100 mm and 150 mm depth. These thermocouples measure the temperature increase at the PIRs during the fire test.

3 rows of thermocouples were introduced vertically at the mid-width into the slab, at 500 mm, 1500 mm and 2440 mm from the wall respectively. Each row was composed of 5 thermocouples positioned respectively at 10 mm, 20 mm, 30 mm, 70 mm and 100 mm from the fire exposed surface of the slab. These thermocouples measure the temperature increase inside the slab during fire exposure.

The gas temperature inside the oven was controlled by 6 pyrometer plates positioned below the test specimen.

#### 3.1.2 Displacement measurements

The measurement of the vertical displacement of the slab during the test was carried out using three wire displacement sensors attached to the slab at 2600 mm from the wall and at 500 mm, 1000 mm and 1500 mm from the lateral side of the slab (Figure 1). These displacement sensors were attached to a metal beam positioned above the test specimen allowing the measurement of the relative displacement of the slab against the concrete frame.

In addition to displacement sensors, a stereo digital images correlation system positioned above the test specimen was used to measure displacements over the whole test specimen during the fire test.

### 3.2 Test description

The test specimen was positioned on the top of the furnace. The wall and the partition wall of the furnace were positioned at the same level in order to reproduce a fire situation in a real cantilever slab connected to a wall using post-installed rebars. In fact, this wall position allows to avoid the formation of a shadow inside the furnace which may disturb the radiative heat transfer and hence could modify the temperature increase inside the test specimen. The cantilever concrete slab was mechanically loaded by a 325 kg dead weight, centered and positioned at 2200 mm from the wall (Figure 1) and then thermally loaded by ISO fire 834-1 (3) until its failure.

$$\theta_{gas}(t) = 20 + 345 \cdot \log_{10}(8 \cdot t + 1) \quad (3)$$

Where  $\theta_{gas}$  is gas temperature in the furnace [K]  
 $t$  is the time of fire exposure [min]

## 4 Results and discussion

### 4.1 Experimental observations

The slab mechanically loaded has been set as the reference state in the rest of this study. The time  $t=0$  is considered as the time of the ignition of the furnace burners. Indeed, the mechanical loading of the cantilever slab induced by the dead weight had generated a vertical downward displacement equal to -5.8 mm. This displacement is composed of a mechanical displacement due to the bending of the slab under the loading effect and of a geometrical displacement due to the angle created by the slip of the rebars. Therefore, the vertical displacement of the slab under mechanical load will not be taken into consideration in the rest of this study.

After few minutes of fire exposure, a vertical upward displacement of the slab was observed due to a thermal curvature (Paragraph 4.2). The failure occurred after **1h57min** of fire exposure caused by the bond failure and the fall of the slab inside the furnace.

### 4.2 Thermal analysis

Thermal profiles recorded by the thermocouples inserted inside the wall (Figure 6.a) show a non-uniform distribution of temperature along the chemically-bonded rebars. Indeed, the heating of the slab generated a thermal gradient at the PIRs. The top of the embedded part of the rebars presented the highest temperatures while the end of the embedded part has the lowest temperatures. The maximum temperature was recorded at the top of the PIR by TC1 and was equal to 89°C, reached at the moment of the slab collapse.

The comparison between measured and calculated thermal profiles shows that calculated temperatures are higher than measured temperatures. This difference between thermal profiles can be explained on one hand by the use of the materials thermal properties provided by EC2<sup>10</sup> for temperature calculations, which leads to an overestimation of temperatures due to the safety aspect of EC2. On the other hand, this difference may be attributed to the non-consideration of the thermal

bridge coming from the steel rebars prolonged inside the slab (Figure 1) when measuring temperatures with thermocouples. In fact, thermocouples measure only the temperature of the concrete wall, and therefore do not consider the contribution of the steel rebars in the heat transfer. Consequently, the PIR temperatures measured by thermocouples should be underestimated.

Similarly, the calculated temperatures in the slab (Figure 6.b) were higher than temperatures measured using vertical lines of thermocouples due to the use of EC2 parameters in thermal calculations which leads to overestimate the temperature profiles.

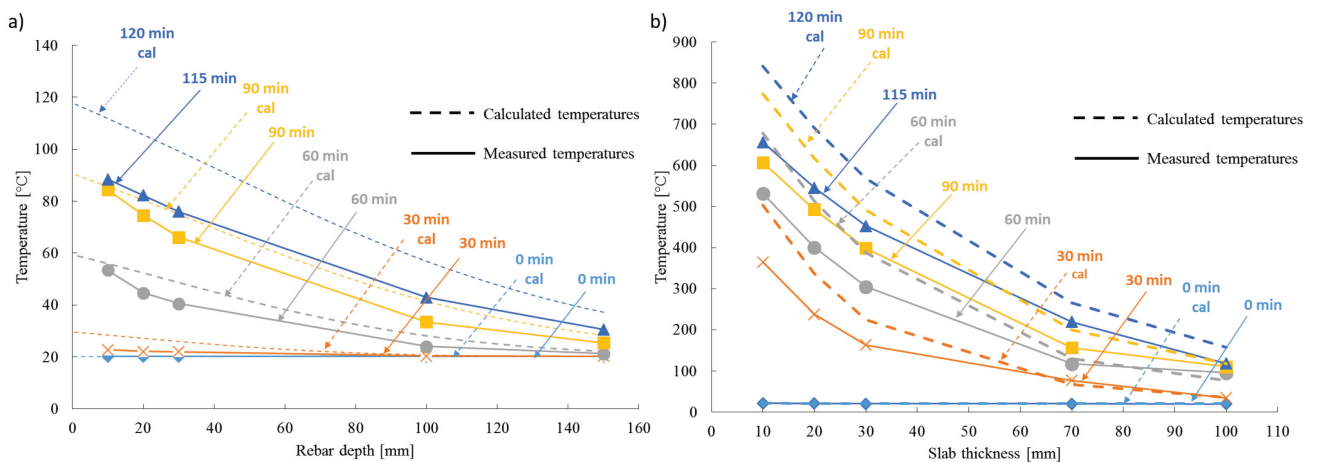


Figure 6: Experimental and numerical temperature profiles. a) At the rebars. b) In the slab

### 4.3 Displacement analysis

Displacements recorded by wire displacement sensors (Figure 7) highlighted a thermal curvature manifested by an upward displacement of the slab since the first minutes of fire exposure. This phenomenon appears due to a differential thermal expansion between the fire exposed and non-exposed surfaces of the concrete slab. Indeed, the concrete directly exposed to fire had expanded under the heat effect, while the concrete non-exposed to fire expanded very little. The difference in thermal expansions had led consequently to the curvature of the slab. As the rotational movements of the slab in the side of the wall were blocked by the chemically-bonded rebars, the free part of the slab has curved and raised upward.

The maximum measured value of vertical displacement due to the thermal curvature was +18.7 mm reached after 28 minutes of exposure to ISO Fire 834-1 ( $\theta_{\text{gas}}(28\text{min})= 832^{\circ}\text{C}$ ). Beyond 28 min of fire exposure, the slab started falling slowly inside the furnace. The zero value of vertical displacement was reached again after 92 min of fire exposure. The downward displacement of the slab could be explained by the decrease of the concrete elastic modulus and basically by the progressive decay in the load bearing capacity of post-installed rebars as a result of temperature increase.

Starting from 109 min of fire exposure, the decay in the bearing capacity of the PIRs had become more and more important and the slab failed more quickly inside the furnace until the total bond failure at **117 min** of fire exposure.

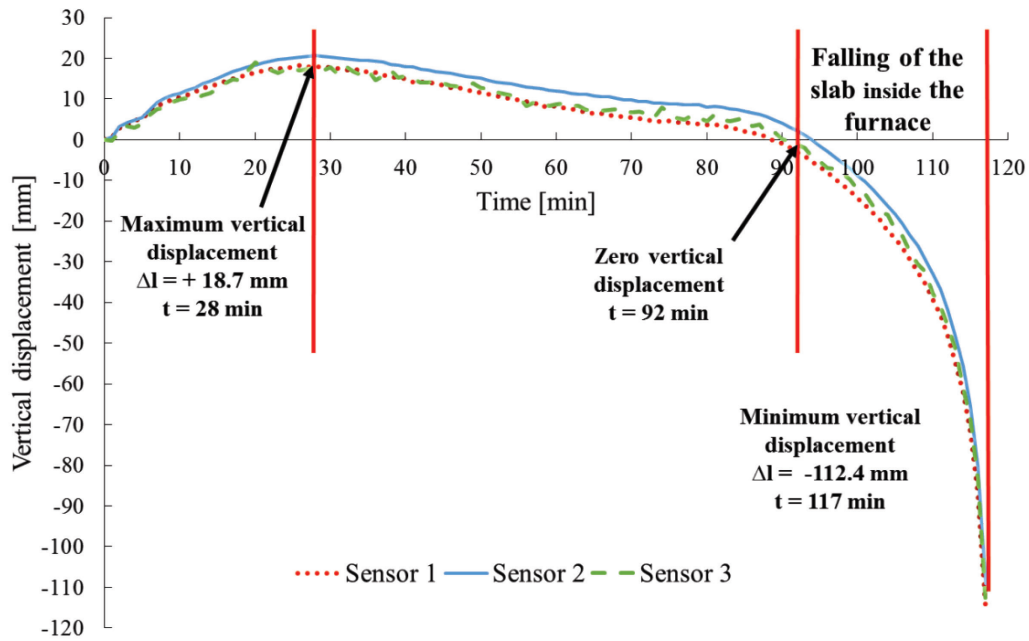


Figure 7: Vertical displacement evolution during the fire test

Displacements recorded by wire displacement sensors during the fire test showed that displacements measured by the sensor positioned at the mid-width of the slab (sensor 2) were slightly greater than displacements measured by the two lateral sensors which indicated sensitively identical values. These displacement values signify that the concrete slab was curved under the thermal effect in a symmetrical manner to an axis passing through its mid-width plan. This interpretation was confirmed by analyzing the results obtained from the stereo digital images correlation system (DIC) which had shown that under the thermal effect, the vertical displacement fields were concentric, which means that the slab had curved symmetrically in its center (Figure 8).

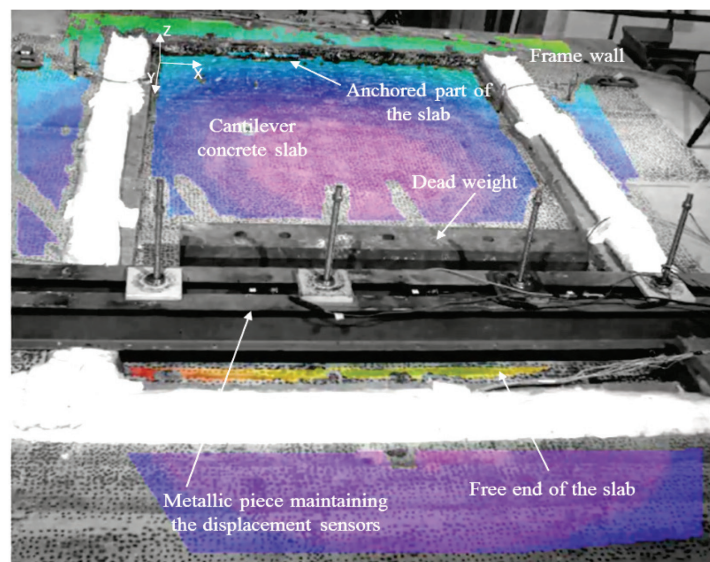


Figure 8: Fields of vertical displacement recorded by DIC during the fire test

#### 4.4 Time of collapse predicted by the EAD 330087-00-06.01 method

The design method proposed by the European Assessment Document 330087-00-06.01<sup>7</sup> for PIRs relies on the same method as the one described in paragraph 2.2. Indeed, the EAD considers that the bond resistance-temperature relationship can be described with an exponential trend curve ( $f_{b,m}=a.exp(-b.\theta)$ ), to which a temperature reduction factor is applied in order to secure the use of PIRs in fire situation. The bond resistance-temperature curve is cut at 17.2 MPa for a C45/55 concrete, in case the bond resistance exceeds 17.2 MPa (Figure 9). For bond resistance values lower than 17.2 MPa, a proportional reduction factor is applied, justified by the conservative assumption that a PIR cannot present higher performances than a cast-in-rebar (covered in the Eurocode). The method of determining the temperature reduction factor  $k_{fi}(\theta)$  is described by equation (4). The variation of  $k_{fi}(\theta)$  with temperature is represented in Figure 10.

$$\begin{cases} k_{fi}(\theta) = \frac{f_{b,m}(\theta)}{f_{b,m,req,d}} \leq 1.0 \text{ for } 20^{\circ}\text{C} \leq \theta \leq \theta_{max} \\ k_{fi}(\theta) = 0 \end{cases} \quad (4)$$

Where  $k_{fi}(\theta)$  is the temperature reduction factor

$f_{b,m}(\theta)$  is the mean bond resistance at temperature  $\theta$

$f_{b,m,req,d}$  is the required bond strength in cold state (= 10 MPa)

$\theta$  is the temperature of the bond

$\theta_{max}$  is the maximal temperature measured during the test

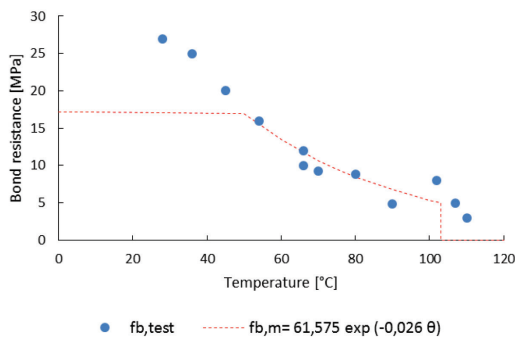


Figure 9: Bond resistance-temperature relationship according to the EAD 330087-00-06.01

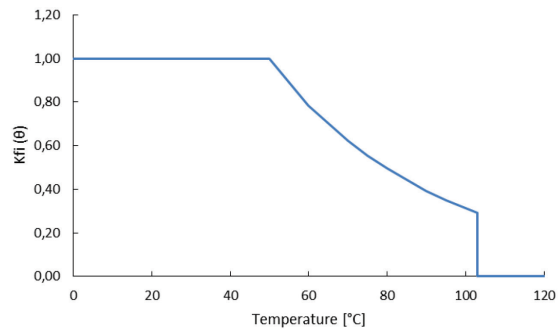


Figure 10: Variation of the  $k_{fi}(\theta)$  with temperature

The design bearing capacity of PIRs in fire situation can be determined from the temperature reduction factor using the characteristic bond resistance at ambient temperature. This characteristic resistance  $f_{bd}$  is equal to 4 MPa in the case of C45/55 concrete, multiplied by a safety factor  $\eta_{fi}$  equal to 1.5. Thus, the bond resistance of the PIR in fire situation is determined according to the value of the temperature reduction factor, as described in equation (5).

$$f_{bd,fi}(\theta) = \eta_{fi} \cdot k_{fi}(\theta) \cdot f_{bd} \quad (5)$$

Where  $f_{bd,fi}(\theta)$  is the bond resistance corresponding to a bond temperature  $\theta$

$f_{bd}$  is the characteristic value of the bond resistance (=4MPa for C45/55 concrete)

$\eta_{fi}$  is the reduction factor for the design load level for the fire situation (=1.5)

$k_{fi}(\theta)$  is the temperature reduction factor

Results show that the calculated load bearing capacity of the PIRs is 4.5 times lower than that obtained by the design method presented in paragraph 2.2. The EAD design method supposes that the structure is not capable to resist to the applied tensile load even at ambient temperature, while the experimental test showed that the structure resisted to 117 minutes of ISO fire exposure. The design of the PIRs according to the EAD<sup>7</sup> method requires a minimum embedment length equal to  $L=225$  mm to ensure 2 hours of fire resistance under ISO 834-1 fire exposure. However, the design method presented in paragraph 2.2 shows that for an embedment length  $L=225$  mm, the slab would be able to resist to 210 min of ISO 834-1 fire exposure. Hence, these results highlight that the safety coefficients applied on the EAD design rules are very strict and should be revised.

#### 4.5 Failure mode analysis

The fractography analysis showed the presence of a mixed failure mode along the bonded part of the rebars as shown in Figure 11. A resin/ concrete interface failure mode was observed at the top of the bonded rebars, up to the two thirds of the embedment length, while the last third of the embedded part of the PIRs presented a steel/resin interface failure mode. This mixed failure mode is the result of a significant thermal gradient present at the PIR at the moment of failure and indicates that the ruin had mainly occurred due to the resin glass transition which led to a significant decay in the load bearing capacity.

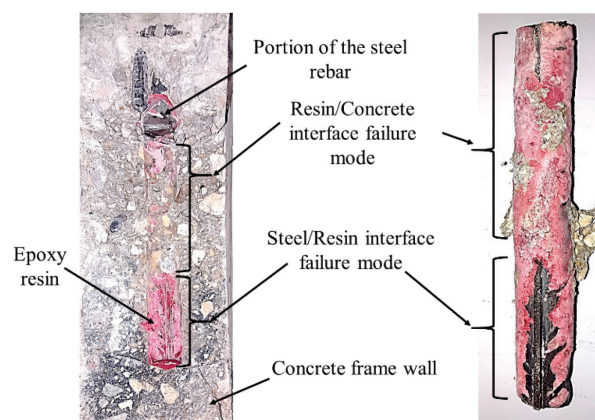


Figure 11: Failure profile observation after the fire test

## 5 Conclusion

This paper presented a full-scale fire test carried out on the CSTB modular gas furnace “Vulcain” in order to validate a fire resistance prediction method for chemically-bonded post-installed rebars. From this study it can be concluded that:

- The proposed method is based on the calculation of the PIRs temperature and on the knowledge of the variation of the bond resistance under the thermal effect.
- The fire test highlighted the presence of a thermal curvature of the slab symmetrically to its mid-width plan and showed that the failure was caused by the slip of the PIRs

- The slab failure occurred after 1h 57 minutes of ISO Fire 834-1 exposure, i.e. only 3 minutes before the fire resistance duration predicted by the model. This result confirms the accuracy of the calculation method in predicting the fire resistance duration of post-installed rebars and shows that the established assumptions are in good agreement with the reality. The comparison with the design method proposed by the EAD 330087-00-06.01<sup>7</sup> showed that the EAD largely underestimates the fire resistance of PIRs. Therefore, the used safety factors are very strict and should be revised.
- The fractography showed the presence of mixed failure mode along the PIR indicating that the resin glass transition was responsible for the slab collapse.

### References:

1. A. F. Bingöl et R. Gül, “Residual bond strength between steel bars and concrete after elevated temperatures”, *Fire Safety Journal*, vol. 44, pp. 854-859, 2009.
2. N. Pinoteau, P. Pimienta, T. Guillet, P. Rivillion et S. Rémond, “Effect of heating rate on bond failure of rebars into concrete using polymer adhesives to simulate exposure to fire”, *Int Adhes Adhes*, vol. 31(8), pp. 851-861, December 2011.
3. H. Sato, K. Fujikake et S. Mindess, “Study on dynamic pullout strength of anchors based on failure modes”, *13th World Conference on Earthquake Engineering*, vol. 854, August 1-6, 2004 Vancouver, B.C., Canada.
4. L. Bouazaoui et A. Li, , “Analysis of steel/concrete interfacial shear stress by means of pull out test”, *International Journal of Adhesion and Adhesives*, vol. 28(3), pp. 101-108, 2008.
5. E. Nigro, A. Bilotta, G. Cefarelli, G. Manfredi et E. Cosenza, “Performance under fire situations of concrete members reinforced with FRP rods: Bond models and design nomograms”, *Journal of composites for construction*, vol. 16(4), pp. 395-406, August 2012.
6. T. Bickel et A. Shaikh, “Shear Strength of Adhesive Anchors”, *Precast Concrete Institute Journal*, pp. 92-100, 2002.
7. EOTA, EAD 330087-00-0601, Systems for post-installed rebar connections with mortar, n°1 EOTA 14-33-0087-06.01, July 2015.
8. Construction Fixings association, CFA Guidance Note: Fixings and Fire, August 1998.
9. CEN. (2002). EN 1991-1-2. Eurocode 1, Part 1-2: Actions on structures: general actions – actions on the structures exposed to fire. Brussels, Belgium 2002.
10. CEN. (2005). EN 1992-1-2 Eurocode 2. Part 1-2: Design of concrete structures - General Rules – Structural fire design. Brussels, Belgium 2005.